Effective electrostatic charge of coagulation factor X in solution and on phospholipid membranes: implications for activation mechanisms and structure–function relationships of the Gla domain

Maria P. McGEE*[1], Hoa TEUSCHLER* and Jie LIANG†

*Medicine Department, Rheumatology Section, Bowman-Gray School of Medicine, Wake-Forest University, Winston-Salem, NC 27157, U.S.A. and †National Center for Supercomputing Applications, University of Illinois at Urbana-Champaign, Urbana, IL 61807, U.S.A.

Electrostatic interactions during activation of coagulation factor X were analysed by comparing effects of ionic strength on reaction rates with predictions of classical electrostatic theory. Geometrical correlations were investigated using alpha-shape-based computations on the crystal structure of Ca–fragment 1 of prothrombin. The ionic strength of the reaction environment was controlled with different univalent salts including NaCl, KCl, CsCl, LiCl, NaI, NaBr and KI. Reactions were assembled in three different environments: aqueous phase, cell membranes and synthetic TF/PS/PC (tissue factor relipidated in 30% phosphatidylserine, 70% phosphatidylcholine) vesicles. Reaction rates were measured at pH 7.2, 4 mM $CaCl_2$ and 33 °C, using chromogenic substrate to follow factor Xa generation. Rates decreased with increasing concentration of univalent salt, and the magnitude of the decrease was independent of salt type. On the basis of electrostatic relationships on PS/PC vesicles, the effective charge on factor X was +1.5, and the PS/factor X stoichiometry was 2.28. Structural analysis of the γ-carboxyglutamic acid (Gla) domain revealed three surface pockets, forming potential sites for Ca^{2+} binding, with distinct spatial orientations. Interpreted together, the results of the geometric analysis and the measured effective charges suggest an efficient electrostatic mechanism for capture and retention of substrates by procoagulant membranes. Non-specific and delocalized interaction between the membrane and each one of the charged facets of the Gla domain can increase the probability of substrate binding, while allowing rotational and translational mobility of substrate for specific interaction with the enzyme.

INTRODUCTION

Previous studies on blood coagulation reactions suggested a dependence of reaction velocity on the electrostatic parameters of substrates and procoagulant membranes [1–5]. Experiments with model peptides [6,7] and cytochrome *c* [8,9] demonstrated that classical electrostatic theory [10–14] is applicable to interactions between charged proteins and phospholipid membranes.

Factor Xa (activated factor X) is one of the key proteases participating in the sequence of specific reactions leading to the coagulation of blood. It is generated from its zymogen form, plasma factor X, by specific limited proteolysis. The reaction is catalysed by either factor VIIa–tissue factor (TF) (extrinsic protease complex) or factor IXa–factor VIIIa (intrinsic protease complex). In these complexes, factors IXa and VIIa carry the catalytic site, and TF and factor VIIIa are cofactors [15,16]. Factor X-activating reactions achieve biologically relevant rates when enzyme complexes are assembled on negatively charged membranes. In addition to negatively charged phospholipids, γ-carboxyglutamic acid (Gla) residues on both substrate and enzyme(s) and the presence of Ca^{2+} ions are necessary for efficient activation [17–19].

The highly conserved Ca^{2+}-binding Gla domain of coagulation proteins has been shown to be indispensable for functional interaction between these proteins and lipid membranes. Structural information on the Ca^{2+}-bound Gla domain of coagulation proteins suggests a complex role for Ca^{2+}. Results from both X-ray crystallography and biochemical studies are consistent with Ca^{2+} bridges between Gla residues and negative charges on the membrane. The number of exposed Ca atoms in the Gla domain structure is lower than the number of bound Ca atoms determined by biochemical measurements [19–23].

We now analyse the electrostatic component of factor Xa-generating reactions using salt-titration experiments and alpha-shape-based geometrical analyses [24–27]. Electrostatic theory provides analytical equations to determine the effective charges operating during the reaction. Computational geometry provides objective and reproducible identification of surface features in the three-dimensional structure of the Gla domain. Results show that electrostatic parameters are different for reactions on natural membranes from those in either aqueous phase or phosphatidylserine/phosphatidylcholine (PS/PC) vesicles. Quantitative alpha-shape-based measurements on prothrombin fragment 1 suggest additional Ca^{2+}-binding sites and a geometrical explanation for the discrepancy between effective and nominal charges in coagulation factor X. On the basis of these results, a model is proposed for the electrostatic interaction between coagulation substrates and lipid membranes.

EXPERIMENTAL

Cells and cell culture

Mononuclear cells from human peripheral blood were enriched for monocytes as previously described [28,29]. The human

Abbreviations used: TF, tissue factor; PC, phosphatidylcholine; PS, phosphatidylserine; PE, phosphatidylethanolamine; PI, phosphatidylinositol; Sph, sphingomyelin; Gla, γ-carboxyglutamic acid.

[1] To whom correspondence should be addressed.

monocytoid cell line THP-1 was obtained from the American Type Culture Collection (Rockville, MD, U.S.A.) and maintained in continuous suspension cultures by weekly passages in M199 culture medium, supplemented with 10 % fetal calf serum. Expression of TF was induced in monocytes and THP-1 cells by stimulation with bacterial lipopolysaccharide (1 μg/ml) in serum-free M199 medium supplemented with 2 % low-protein serum replacement (Sigma Chemical Co., St. Louis, MO, U.S.A.). Viability of cells was monitored by Trypan Blue dye exclusion in representative experiments. The viability of THP-1 cells decreased 15–40 % during 3–20 h of culture in serum-free medium, but monocyte viability remained more than 90 %.

Natural and artificial membrane vesicles

Membranes shed by THP-1 cells during culture were collected by differential centrifugation and filtration through filters of 0.4 μm pore size. Representative preparations of cells and vesicles were processed for phospholipid quantification and composition as before [30,31]. The phospholipid composition was phosphatidylethanolamine (PE) (22.3 %), phosphatidylinositol (PI) (3.8 %), PS (12.1 %), PC (50.6 %), and sphingomyelin (Sph) (7.7 %) and PE (31.0 %), PI (4.4 %), PS (12.0 %), PC (39.5 %) and Sph (10.3 %) for THP-1 cells and monocytes respectively. The phospholipid composition of vesicles shed by THP-1 cells was PE (34.3 %), PI (5.7 %), PS (13.0 %), PC (36.3 %) and Sph (7.4 %). The molar ratio cholesterol/phospholipid was approx. 1:3 and similar for monocytes and THP-1 cells. The total phospholipid content was 4 and 11 nmol/10^6 cells for monocytes and THP-1 cells respectively. The total phospholipid content of vesicles shed by THP-1 cells during incubation was 0.78 nmol/10^6 cells. The differences in phospholipid distribution among monocytes, THP-1 cells and THP-1 vesicles were within the range of experimental variation expected from TLC determinations with different preparations of the same membrane. Lipid determinations were performed by Martha Kennedy at the Lipid Analyses Core Laboratory, Comprehensive Cancer Center, Bowman Gray School of Medicine. The size of cells and particles was determined by electron microscopy in samples prepared as before [28]. Natural lipid vesicles were ellipsoid in shape with 0.186 ± 0.06 and 0.225 ± 0.07 μm (means $\pm$ S.D.) minor and major axis respectively, as determined from 100 measurements in microphotographs of vesicles magnified 50 700-fold. Monocytes and THP-1 cells were spherical with 6.9 ± 0.17 and 5.6 ± 1.6 μm radius respectively. TF antigen was measured by enzyme immunoassay in representative samples of monocytes. Functional chromogenic assays were used to estimate relative amounts of TF on THP-1 cells and vesicles [29].

Recombinant TF (American Diagnostics) was incorporated into a 30:70 PS/PC (Avanti Polar Lipids) mixture as described [32]. From previously published electromicrographs [33], the average size of these types of vesicle is within the range determined for natural vesicles isolated from THP-1 cells. The relative molar ratio of TF protein to phospholipid used in our preparation was 1:4125.

Measurement of reaction rates

Rates of factor Xa generation were measured in reaction mixtures with fixed concentrations of TF (0.02–2 nM, depending on the type of experiment), factor VIIa (4 nM), Ca^{2+} (4 mM) and various concentrations of different univalent salts. Reaction mixtures were buffered with Tris buffer, pH 7.2, containing ovalbumin at 0.5 mg/ml, and equilibrated at 33–35 °C. Concentrations of factor VIIa used were saturating for TF both on membranes and in solution. (It has been shown previously that the dissociation constant for TF–factor VIIa interaction is not significantly modified by changes in ionic strength [3].) Reactions were initiated by the addition of factor X and rates determined from the change in factor Xa concentration in six sequential samples taken at 0.5–2.0 min intervals. The concentration of factor Xa in each sample was determined from the initial rate of chromogenic substrate hydrolysis (methoxycarbonyl-D-cyclohexylglycyl-glycyl-arginine-*p*-nitroanilide acetate) as before [34]. The concentration of factor X was within the physiological range and less than the apparent dissociation constant of factor X for either PS/PC or biological membranes [35]. Maintaining the factor X concentration below saturation was important to ensure that the fraction of occupied membrane sites remained low, and that reaction rates changed with substrate concentration within the range of ionic strength tested in these studies. This latter condition was demonstrated in salt-titration experiments with factor X concentration fixed at either 85 or 360 nM. For measurement of factor Xa generation by the intrinsic pathway protease, reaction mixtures were identical, except that factor VIIa was replaced by factors IXa and VIII (1 nM each). Factor VIII was preactivated with thrombin as before [28,34]. Titrations with NaCl under each set of conditions described in the following sections were repeated three to six times. Titrations with other univalent salts were repeated two to three times.

Coagulation factors

Recombinant human factor VIIa was a gift from Ulla Hedner (Novo Nordisk). Recombinant human TF was purchased from American Diagnostics. Human factors X and IX were from Enzyme Laboratories, South Bend, IN, U.S.A., and immunopurified human factor VIII (Monoclate) was purchased from Armour Pharmaceutical Company (Kankakee, IL, U.S.A.).

Computational geometry [24–27]

The geometrical characteristics of the Gla domain were analysed using automatic unbiased computations based on the alpha-shape algorithm [24]. The algorithm was applied to the crystal structure of Ca–prothrombin fragment 1 (residues 1–156 of prothrombin; Brookhaven Protein Data Bank, reference 2PF2) [22], with the software programs VOLBL, INTERSECT and POCKET. These programs are available from the National Center for Supercomputer Applications, University of Illinois at Urbana, Champaign. The alpha-shape algorithm generates a one-parametric family of shapes from available three-dimensional co-ordinates of X-ray-crystallography models [25]. This approach has distinct advantages over methods based on visual inspection of molecules. In particular, geometrical features of complex structures are identified automatically in a reproducible and objective manner from three-dimensional data. In contrast, previous approaches relied primarily on subjective interpretation of manually rotated graphic renditions. The alpha-shape-based method is analytical and faithful to the information contained in the atomic co-ordinates deduced from the crystal. Therefore this approach does not address the possibility that some of the geometrical properties of the crystal structure may be irrelevant to function.

Theoretical considerations

Long-range electrostatic forces that mediate interactions between charged molecules are influenced by the concentration of

ionizable salts in the reaction environment. Equations relating the dependence of reaction rates and binding constants on ionic strength have been derived on the basis of classical electrostatic theory [10–14]. The presence of salts modifies the activity coefficients of charged reactants and consequently the rate and equilibrium constants [10]. In the present studies, the interaction between substrate, S, and enzyme, E, (or between substrate and membrane) is assumed to result in the formation of a critical complex, B, with charge equal to the sum of the effective charges carried by the reactants. The concentration of the critical complex, [B], is assumed to be proportional to the concentration of substrate-binding sites, [E], on either the enzyme or the membrane and to the concentration of substrate, [S], in regions adjacent to the binding sites

$$[B] = p[E][S] \quad (1)$$

where p is a proportionality constant. The average concentration of charged substrate near its interaction site can be calculated from the bulk substrate concentration, [Sb], taking into account the mean electrostatic potential, ψ, at a distance r, described by the Debye–Huckel derivation using the linearized Poisson–Boltzman distribution equation:

$$[S] = [Sb]\exp(-\psi ez/kT) \text{ and } \psi \sim ze\exp(-\kappa r)/(4\pi\epsilon_a\epsilon_0 r) \quad (2)$$

where e is the unit charge, z the valence, k the Boltzman constant, T the temperature (K), $e\epsilon_a$ the dielectric constant of the medium and ϵ_0 the permittivity of space. The screening term $\exp(-\kappa r)$ includes the Debye length, $\kappa^{-1} = [(\epsilon_0\epsilon_a kT)/2z^2e^2C]^{1/2}$ where C is the number of ions per volume. At infinite dilution, κ approaches 0. By definition, for any species, the activity coefficient, f, is the ratio between the activity (or effective concentration) in the infinitely diluted solution and the activity in the real solution; therefore, in the case of reactants and critical complex,

$$\ln f_s f_e/f_c = \ln[S^0][E^0]/[B^0] - \ln[S][E]/[B] \quad (3)$$

where the superscript 0 refers to the infinitely diluted solution, and f_s, f_e and f_c to the activity coefficients of the substrate, enzyme and complex respectively. The concentration of reactants and critical complex can be related to reaction rate, R (or binding constant K), using Bronsted–Bejerrum expression for activity coefficients [11,12]:

$$R = R_0 f_s f_e/f_c \text{ or } K = K_0 f_s f_e/f_c \quad (4)$$

where R_0 and K_0 are rate and equilibrium constant respectively in an infinitely diluted solution. Combining eqns. (1), (2), (3) and (4) results in the relationship:

$$\ln R = \ln R_0 + 2Az\sqrt{C} \text{ or } \ln K = \ln K_0 + 2Az\sqrt{C} \quad (5)$$

where z is the product between the relevant charges on the reacting species and A is a factor containing known constants. Under the conditions of our experiments, $2A$ has a value of about 2.3.

On membranes, the effect of ionic strength on activity coefficients of reactants can also be examined using Gouy–Chapman equations and similar relationships [6,13]. The dependence of initial substrate binding on ionic strength has been analysed on the basis of derivations that consider changes in electrostatic free energy on binding [8,9,14]. In the high-potential limit

$$K/K' = C^{-(z+Az^2)}L^{2z} \quad (6)$$

where K and K' are the apparent and intrinsic binding constants respectively, L is the fraction of charged phospholipids on the membrane, z is the effective charge on the substrate, and A is a factor containing constants describing the electrostatic self-energy of the substrate and is small for substrates of low effective charge [14]. [Here the term intrinsic binding constant refers to component(s) of the interaction that do not change with ionic strength.]

These theoretical considerations imply that electrostatic effects depend exclusively on charge. Therefore results of salt-titration experiments should be independent of the chemical species of the univalent salt used to control the ionic strength.

RESULTS

Dependence of rate on salt concentration for reactions assembled in aqueous phase

Initial rates of factor Xa generation from factor X (170 nM) by soluble TF/factor VIIa (at 2 and 4 nM respectively) were measured at various concentrations of univalent salt (0.04–0.39 M) with $CaCl_2$ fixed at 4 mM. Rates of factor Xa generation by TF/factor VIIa in aqueous phase decreased with the salt concentration. The logarithm of the rate plotted against either the square root or logarithm of salt concentration gave straight lines as predicted by eqns. (5) and (6). The product of interacting charges, as determined from eqn. (5), was -2.3 ± 0.12. Results obtained with NaCl are illustrated in Figure 1. Salt titrations were repeated with six other univalent salts to exclude the possibility that observed effects were salt-specific. Results with each univalent salt tested were similar, giving slopes not significantly different from the overall average slope (Table 1).

Dependence of rate on salt concentration for reactions assembled on lipid vesicles

Rates of factor Xa generation by TF/factor VIIa on natural lipid vesicles from THP-1 cells were measured under the same conditions as for aqueous-phase reactions. The concentration of TF in these preparations, estimated on the basis of functional measurements and immunoassays on monocyte membranes [29], ranged from 0.02 to 0.1 nM. Salt titrations were also repeated using TF reconstituted on artificial vesicles formed with purified PS/PC mixtures. For comparison, factor Xa generation rates by the intrinsic protease complex factor IXa/factor VIIIa were

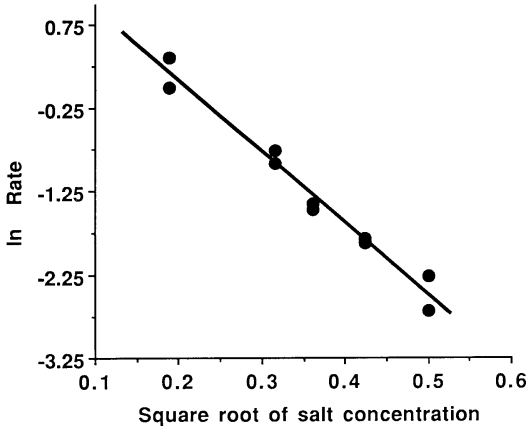

Figure 1 Dependence of factor Xa generation on ionic strength during reactions in aqueous phase and on natural membranes

Initial rates of factor Xa generation in aqueous phase were measured at fixed concentrations of TF (1.7 nM), factor VIIa (4 nM), $CaCl_2$ (4 mM) and factor X (170 nM). Ionic strength was varied between 0.04 and 0.25 with NaCl. Points are rate values from two independent measurements at each salt concentration. Data are plotted according to eqn. (5) (see the Experimental section).

Table 1 Effect of different anions and cations on reactions assembled in the aqueous phase

Rate, R, for factor Xa generation by TF/ factor VIIa in solution was determined at six different concentrations (C; 0.04–0.39 M) of univalent salts listed. All other reagents were kept constant at concentrations indicated in the legend to Figure 1. Linear equations were fitted to data points transformed as $\ln R$ versus $\sqrt{C}$ using computer program Statview 512+. Coefficients of determination, r^2, obtained from regression analyses are indicated for each transform. The coefficient of determination is the ratio of the explained sum of squares over the total sum of squares. It is a conservative statistical measure of the proportion of the total variation that is explained by the theoretical relationship [36]. Results for charge are means ± S.E.M.

Salt	$\text{Charge}_{(\ln R/\sqrt{C})}$	r^2
NaCl	2.3 ± 0.12	0.991
KCl	2.3 ± 0.13	0.990
CsCl	2.5 ± 0.09	0.989
LiCl	2.6 ± 0.26	0.973
NaI	2.7 ± 0.31	0.978
NaBr	3.0 ± 0.29	0.984
KI	2.9 ± 0.32	0.972

Table 2 Effect of ionic strength on factor Xa generation by extrinsic and intrinsic proteases on PS/PC membranes

Rate R, of factor Xa generation on PS/PC membranes with either extrinsic (TF/factor VIIa) or intrinsic (factor IXa/VIIIa) proteases was measured at different concentrations (C; 0.072–0.26 M) of NaCl. The concentration of factor IXa and factor VIII was 1 nM each. Linear equations were fitted to data points transformed either as $\ln R$ versus $\sqrt{C}$ or $\ln R$ versus $\ln C$. Other reagents and data analysis were as indicated in the legends to Figure 1 and Table 1. [Difference between slopes with intrinsic and extrinsic proteases is significant ($P = 0.025$) in a t test for paired data from three different salt-titration experiments.] Results for slope are means ± S.E.M.

Protease	$\text{Charge}_{(\ln R/\sqrt{C})}$	$r^2_{(\ln R/\sqrt{C})}$	$\text{Charge}_{(\ln R/\ln C)}$	$t^2_{(\ln R/\ln C)}$
Extrinsic	3.4 ± 0.246	0.978	1.50 ± 0.162	0.944
Intrinsic	2.1 ± 0.213	0.961	1.04 ± 0.110	0.957

Table 3 Effect of ionic strength on reactions assembled on intact cell membranes expressing different levels of TF

Cells, either monocytoid THP-1 or blood monocytes, were incubated with bacterial lipopolysaccharide to stimulate synthesis and expression of TF. After the indicated time periods, cell suspensions were washed to remove shed membrane vesicles and incorporated in reaction mixtures at a concentration of 2×10^6/ml. Rates were measured at different ionic strength levels (0.072–0.25), while other reagents were kept at the fixed concentrations indicated in Figure 1. The values in the first column correspond to rates at the lowest salt concentration and reflect the relative amount of functional TF protein expressed on the surface. Rates are directly plotted against square root of ionic strength. The slopes and coefficients of determination from linear regression analyses are indicated. Results are means ± S.E.M.

Cells	Rate (nmol of FXa/min)	Slope	r^2
THP-1			
18 h	7.13 ± 0.18	3.0 ± 0.29	0.962
3 h	0.31 ± 0.004	3.7 ± 0.460	0.980
Monocytes			
6 h	0.91 ± 0.08	3.7 ± 0.11	0.996

measured under similar conditions on the same membranes. (For this protease, salt effects may also reflect electrostatic interactions between enzyme components with membrane.) In both natural and artificial vesicles, reaction rates decreased with ionic strength.

Table 4 Interactions between Gla carboxylate oxygens and Ca

Values correspond to van der Waals volume overlaps, in Å^3, of Ca atoms. Overlaps were computed from the X-ray crystal structure of Ca–prothrombin fragment 1 using the alpha-shape-based software program, INTERSECT.

	OE1	OE2	OE3	OE4
Ca-1: Gla-26	0	4.2	3.6	0
Gla-30	4.2	0	3.5	0
Ca-2: Gla-8	0	2.4	0	2.8
Gla-27	0	1.9	0	0
Gla-30	0	0	3.9	3.7
Ca-3: Gla-17	3.6	2.6	0	0
Gla-27	2.6	0	0	0
Gla-30	0	0	0	3.0
Ca-4: Gla-7	2.2	0	0	0
Gla-8	0	0	2.7	0
Gla-17	0.7	0	5.8	0
Gla-27	3.1	0	0	3.2
Ca-5: Gla-7	3.5	3.6	3.4	1.6
Gla-21	0	0	0	2.2
Ca-6: Gla-20	0	3.2	0	0
Gla-21	0	2.8	3.9	0
Ca-7: Gla-15	0	0	0	1.9
Gla-20	0	0	3.8	2.3

For reactions in PS/PC membranes, plots of $\ln R$ versus either $\sqrt{C}$ or $\ln C$ [eqns. (5) and (6) respectively] were linear, with $R^2 > 0.94$ (Table 2). The effective charge on factor X was $+1.50 \pm 0.16$ and $+1.04 \pm 0.11$ on membranes with extrinsic and intrinsic protease respectively. From these values and from the product between charges determined using eqn. (5), the calculated stoichiometry was -2.28 and -2.07 membrane charges per factor X for extrinsic and intrinsic protease respectively.

In contrast, for reactions assembled on natural membranes, logarithmic plots deviated markedly from linearity. Instead, the rate was directly related to the square root of the salt concentration. For this relationship the coefficients of determination were greater than 0.96 and the standard errors of the slopes were less than 15% with each salt type. Deviation from expected relationships suggests that reaction mechanisms on natural membranes are different from those either in aqueous phase or on PS/PC vesicles.

Dependence of rate on salt concentration for reactions on intact cell membranes

To determine if the relationship observed is dependent on the size of the membrane or on the density of the enzyme on the membrane, salt titrations were repeated on intact cells expressing different levels of TF. (Osmotic effects of salts on cell viability were examined in one experiment using the Trypan-Blue-dye-exclusion technique. The proportion of viable monocytes was 81, 79, 82, 88, 83 and 82% for ionic strengths 0.072, 0.102, 0.129, 0.150, 0.202 and 0.262 respectively.) Analysis of salt-titration data indicated that reaction rates on intact cells, as on cell vesicles, were better described by a linear relationship between rate and $\sqrt{C}$ than by eqns. (5) and (6). Since the cell diameter is at least 60 times larger than the diameter of the vesicles, within these limits, the overall size of the membrane does not appear to be an important factor affecting the observed deviation from predicted relationships. (However, because cell membranes present many pseudopodia and invaginations, this experiment does not exclude the possibility that reactive regions on the intact cell membrane had curvatures similar to that of vesicles. Further, the

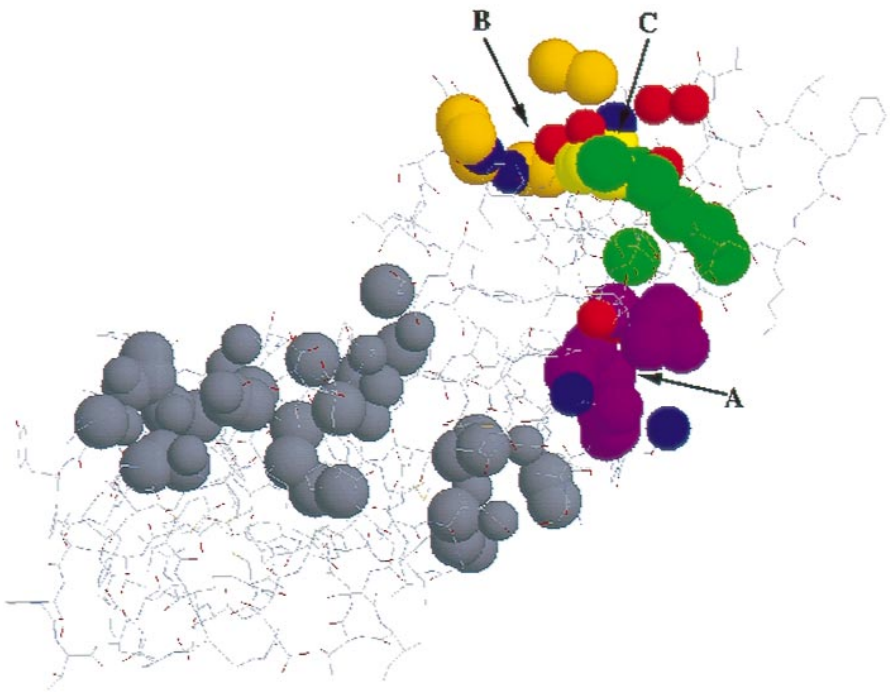

Figure 2 Pockets on the Gla domain of Ca–prothrombin fragment 1

Atoms lining the nine pockets identified in the Ca–prothrombin fragment 1 are in space-filling 'balls' and superimposed on the 'stick' rendition of Ca–prothrombin fragment 1. The three pockets in the Gla domain are indicated by arrows that point to the distinct spatial orientation of the pocket entrances. Amino acid residues that contribute atoms to these three pockets are listed in Table 5. Ca atoms are shown in green, N in blue and O in red. Carbon atoms are in purple for pocket A, mustard for pocket B and yellow for pocket C.

Table 5 Molecular pockets containing Ca and/or atoms from Gla residues

The pockets were computed from the X-ray structure of Ca–prothrombin fragment 1 using the alpha-shape-based software package POCKET. Location, orientation and relative dimensions of these pockets in the structure are illustrated in Figure 2.

Pocket A	Pocket B	Pocket C
O from Gla-20, C-18, L-19, R-52	O from Gla-30, G-12, A-31	Ca-3
NH1 from R-52	N from Gla-33(?), G-12, L-32	OE4 from Gla-8, Gla-30
ND2 from N-53	C from Gla-33(?), K-11, A-31, L-32	OE2 from Gla-30
C from Gla-21, Gla-20, L-19, P-22, R-52, R-55, L-58		O from Gla-8, R-10, Gla-7
		N from G-12
		C from Gla-30, G-12, Gla-8

membrane structure may also change in response to hypo- or hyper-tonic medium.) The mechanism was also independent of the density of TF expressed by the cells (Table 3) and of the total cell concentration in the reaction mixture. Salt titrations with cells at 0.6×10^6, 1.3×10^6 and 2.6×10^6/ml resulted in direct linear relationships. Under every condition, coefficients of determination for the R versus $\sqrt{C}$ linear relationships on cells were higher than 0.96.

Atomic environment and geometrical features of Ca and Gla carboxylate oxygen atoms

The structure of the Gla domain of prothrombin fragment 1 crystallized in the presence of Ca^{2+} has been described in extensive detail by other investigators [22]. In the present analysis, specific aspects of the structure are examined from a geometric perspective using new computational approaches not available at the time of the previous studies. In particular, the surface texture and spatial orientation of putative membrane-binding region(s) of the Gla domain are evaluated to identify features that may help to interpret and correlate structure with data on electrostatic parameters and with previous biochemical information [19]. The solvent exposure of Ca atoms and carboxylate oxygen atoms was measured using the alpha-shape-based software program VOLBL. The interactions between carboxylate oxygen atoms and Ca were determined quantitatively by computing direct van der Waals contact volumes with the program INTERSECT. This software does not rely on measurements of distances; instead it rigorously computes the contact volumes. This is particularly important in situations in which Ca and carboxylate oxygen atoms may be within a short distance but separated by a third atom and therefore with no direct volume overlap. Volume

overlaps are indicated in Table 4. The Ca atoms ranked on the basis of dual criteria (from largest to smaller exposed surface, and from lowest to higher volume overlap) follow the order Ca-7, Ca-6, Ca-5, Ca-3, Ca-1, Ca-2 and Ca-4. In this sequence, Ca-7 would be the most and Ca-4 the least likely of the Ca atoms in the Gla domain to form additional interactions. Similarly ranked, the carboxylate oxygen atoms from Gla residues follow the order Gla-20, Gla-26, Gla-15, Gla-21, Gla-8, Gla-7, Gla-30, Gla-27 and Gla-17. (Gla-33 was excluded from this analysis because the side-chain atoms appear to be disordered.) The surface texture of the Gla domain was analysed using the software package, POCKET [37]. This new alpha-shape-based approach computes analytically those rugosities, cavities and/or indentations with outlets narrower than the concavities. It automatically localizes possible binding-site pockets in molecules. The computations identified a total of nine pockets in the Ca–prothrombin fragment 1 structure. Three of the pockets (A, B and C; Figure 2) were in the Gla domain and included atoms from Gla residues and/or Ca atoms (Table 5). Pockets A and B are lined by atoms that have either negative or neutral partial charge. Pocket C is partially lined by carboxylate atoms OE4 from Gla-8 and Gla-30 and OE2 from Gla-30, and by Ca-3. All three pockets are large enough to contain at least one additional Ca atom. The opening of each pocket faces a different direction in space.

DISCUSSION

The rate of factor Xa generation by TF/factor VIIa, assembled either in aqueous phase or on lipid membranes, changed with ionic strength. The changes were independent of the type of univalent salt used to control the ionic strength, indicating that the observed effect was electrostatic. Consequently results demonstrate that electrostatic forces are a significant component of the reaction both in aqueous media and on lipid membranes. However, the relationship between ionic strength and rate was different for reactions in aqueous phase and PS/PC membranes from those on biological membranes. In aqueous phase and on artificial PS/PC membranes, the logarithm of the rate changed linearly with both the square root and the logarithm of ionic strength. These relationships are as predicted by classical electrostatic theory for direct interactions between charged reactants in solution and for interactions between charged substrates and membranes respectively. The electrostatic effect on natural membranes was better described by a linear relationship between the rate and the square root of the univalent salt concentration. These results suggest that mechanisms of reactions assembled on natural membranes involve different step(s) from those of reactions in aqueous phase or on PS/PC membranes. This interpretation is consistent with previous kinetic evidence for surface transfer of substrate as the rate-limiting step on procoagulant membranes with high affinity for substrate [34,35,38,39].

Electrostatic theory in the simple form applied here invokes assumptions about the magnitude of surface potential and charges on the membrane. The applicability range of either low- or high-potential approximation of the theory has been estimated [14]. For the range of salt used and the proportion of negatively charged lipid in these membranes, the error expected from using either the low- or high-potential approximation is between 5 and 20%. Therefore, within these limits, salt-titration experiments also provided quantitative information on effective charges during factor X activation reactions.

Net interacting charges during activation by TF/factor VIIa on PS/PC membranes were 1.5 positive charges on factor X and 2.2 negative charges on the membrane. The value for membrane charges is lower than the previously reported stoichiometry of 5 between PS/PC membranes and factor X, obtained from direct binding titrations ([19] and the following three papers in the series). The value of effective charge on factor X obtained does not correspond to the actual physical charges deduced from the structure of the Ca- Gla domain. The apparent reduction in charge of interacting proteins can be explained by considering their size, average number of ionic contacts during micro-collisions and spatial orientation of the charges [40,41].

Exposed charges in the Gla domain, including three additional pockets with potential for Ca^{2+} binding, are located on three different facets of the structure (Figure 2). It is unlikely that these three facets can make simultaneous contact with the lipid surface. Pocket A is located below the plane that passes through the seven Ca atoms. Directly 'above' this pocket are Ca-7, Ca-6 and Lys-3. It is possible that one (or two) additional Ca atoms fit into the pocket forming an extensive positively charged face for interaction with the membrane. An additional Ca may also bind into pocket C and co-ordinate with atom OE4 from Gla-8 and OE2 from Gla-30. This Ca together with the exposed surface of Ca-3 in the pocket and the vicinal Ca atoms 1 and 2 can form another positively charged face with a different orientation in space. Similarly, pocket B can provide an additional site for interaction with Ca. Interestingly, with biochemical methods, at least 10 Ca atoms are measured in the substrate–membrane complex. In contrast, only seven Ca atoms are identified in the crystal structure of the Gla domain [19,22]. This further suggests that the three pockets identified by alpha-shape-based analysis may be occupied by Ca during functional interaction of coagulation substrates with membranes.

The non-specific delocalized nature of electrostatic interactions [41–43], interpreted within the geometrical context of alpha-shape-based analyses, suggests an efficient mechanism for coagulation reactions on charged membranes. The three different orientations in space of the potentially interacting facets on the Gla domain greatly improve the chances of coagulation substrate binding to negative charges on membrane. Because electrostatic interaction of each facet is non-specific and delocalized, the substrate on the membrane can maintain the rotational and translational flexibility that is necessary to find the specific line-up orientation with the enzyme complex.

Surface charge density of cell membranes can be modified during pathological processes by a variety of ligands, including coagulation proteins and extracellular matrix components. In this regard, we have previously shown that negatively charged proteoglycans expressed on monocyte surfaces can modulate factor Xa generation reactions [44]. Changes in the density of surface charges on biological membranes may contribute to abnormal coagulation in arteriosclerosis, neoplasia and infectious disease. Electrostatic interactions should also be taken into account when extrapolating kinetic parameters of coagulation reactions on artificial lipid vesicles to complex biological membranes.

We are grateful to Roy Hantgan (Biochemistry Department, Bowman-Gray School of Medicine) for helpful comments and suggestions. This work was supported by NSF MCB 9601411 (to M.P.M.) and by NSF CISE postdoctoral fellowship, grant ACS 94-04900 (to J.L.).

REFERENCES

1 Papahadjopoulos, D., Hougie, C. and Hannahan, D. J. (1962) Proc. Soc. Exp. Biol. Med. **11**, 412–416
2 van Rijn, J. L. M. L., Govers-Riemslag, J. W. P., Zwaal, R. F. A. and Rosing, J. (1984) Biochemistry **23**, 4557–4564
3 Krishnaswamy, S. (1992) J. Biol Chem. **267**, 23696–23706
4 McGee, M. P. and Teuschler, H. (1995) J. Biol. Chem. **270**, 15170–15174

5 London, F. and Walsh, P. N. (1996) Biochemistry **35**, 12146–12154
6 Kim, J., Mosior, M., Chung, L. A., Wu, H. and McLaughlin, S. (1991) Biophys. J. **60**, 135–148
7 Thorgeirsson, T. E., Yu, Y. G. and Shin, Y.-K (1995) Biochemistry **34**, 5518–5522
8 Heimburg, T. and Marsh, D. (1995) Biophys. J. **68**, 536–546
9 Heimburg, T. and Marsh, D. (1996) in Biological Membranes, (Merz, Jr., K. and Roux, B., eds.), pp. 405–461, Birhkhauser, Boston
10 Glasstone, S., Laidler, K. J. and Eyring, H. (1941) The Theory of Rate Processes, 1st edn., pp. 423–429, McGraw-Hill Book Company, New York and London
11 Scatchard, G. (1930) J. Am. Chem. Soc. **52**, 52–61
12 La Mer, V. K. (1932) Chem. Rev. **10**, 179–211
13 Verwey, E. J. W. and Overbeek, T. G. (1948) Theory of Stability of Lyophobic Colloids, Elsevier, Amsterdam
14 Trauble, H., Teubner, M., Woolley, P. and Eibl, H. (1976) Biophys. Chem. **4**, 319–342
15 Nemerson, Y. and Bach, R. (1982) Prog. Hemost. Thromb. **6**, 237–261
16 Kane, W. H. and Davie, E. W. (1988) Blood **71**, 539–555
17 Nelsestuen, G. L. (1988) Current Advances in Vitamin K Research (Suttie, J. W., ed.), pp. 335–339, Elsevier, New York
18 Neuenschwander, P. F. and Morrissey, J. H. (1994) J. Biol. Chem. **269**, 8007–8013
19 Nelsestuen, G. L. and Lim, T. K. (1977) Biochemistry **16**, 4164–4171
20 Jacobs, M., Freedman, S. J., Furie, B. C. and Furie, B. (1994) J. Biol. Chem. **269**, 25494–25501
21 Sunnerhagen, M., Forsen, S., Hoffren, A.-M., Drakenberg, T., Teleman, O. and Stenflo, J. (1995) Nature Struct. Biol. **2**, 968–974
22 Soriano-Garcia, M., Padmanabhan, K., de Vos, A. and Tulinsky, A. (1992) Biochemistry **31**, 2554–2556
23 Nelsestuen, G. L., Broderius, M. and Martin, G. (1976) J. Biol. Chem. **251**, 6886–6993
24 Edelsbrunner, H. and Mucke, E. (1994) ACM Trans. Graph. **13**, 43–72
25 Edelsbrunner, H. (1995) Discrete Comput. Geom. **13**, 415–440
26 Edelsbrunner, H., Facello, M., Fu, P. and Liang, J. (1995) Proceedings of the 28th Annual Hawaii International conference on System Sciences, vol. 5, pp. 256–264, IEEE Computer Society Press, Los Alamitos, CA
27 Edelsbrunner, H. (1987) Algorithms in Combinatorial Geometry, Spring-Verlag, Berlin
28 McGee, M. P., Li, L. C. and Hensler, M. (1992) J. Exp. Med. **176**, 27–35
29 McGee, M. P., Foster, S. and Wang, X. (1994) J. Exp. Med. **179**, 1847–1854
30 Bligh, E. and Dyer, J. W. (1959) Can. J. Biochem. Physiol. **37**, 911–917
31 Rouser, G., Fleisher, S. and Yamamoto, A. (1970) Lipids **5**, 494–496
32 Carson, S. D. (1987) Thromb. Res. **47**, 379–387
33 Slack, J. R., Anderton, B. H. and Day, W. A. (1973) Biochim. Biophys. Acta **323**, 547–559
34 McGee, M. P. and Li, L. C. (1991) J. Biol. Chem. **266**, 8079–8085
35 Scandura, J. M., Ahmad, S. S. and Walsh, P. N. (1996) Biochemistry **35**, 8890–8902
36 Sokal, R. R. and Rohlf, F. J. (1973) Introduction to Biostatistics, W.H. Freeman and Co., San Francisco
37 Edelsbrunner, H., Facello, M. and Liang, J. (1996) Proceedings of the 1st Pacific Symposium on Biocomp, pp. 272–287, World Scientific, Singapore.
38 Giensen, P. L. A., Willems, G. M. and Hermens, W. T. (1991) J. Biol. Chem. **266**, 1379–1382
39 Evans, J. C. and Nelsestuen, G. L. (1994) Biochemistry **33**, 13231–13237
40 Stankowski, S. and Schwarz, G. (1990) Biochim. Biophys. Acta **1025**, 164–172
41 Northrup, S. H., Boles, J. O. and Reynolds, C. L. (1988) Science **241**, 67–70
42 McLaughlin, S., Mulrine, N., Gresalfi, T., Vaio, G. and McLaughlin, A. (1981) J. Gen. Physiol. **77**, 445–473
43 Peitzsch, R. M., Eisenberg, M., Sharp, K. A. and McLaughlin, S. (1995) Biophys. J. **68**, 729–738
44 McGee, M. P., Teuschler, H., Parthasarathy, N. and Wagner, W. D. (1995) J. Biol. Chem. **270**, 26109–26115

Received 15 May 1997/1 September 1997; accepted 8 October 1997